

UC Davis

UC Davis Previously Published Works

Title

Acute Changes in NADPH Oxidase 4 in Early Post-Traumatic Osteoarthritis.

Permalink

<https://escholarship.org/uc/item/02d7z58k>

Journal

Journal of orthopaedic research : official publication of the Orthopaedic Research Society, 37(11)

ISSN

0736-0266

Authors

Wegner, Adam M
Campos, Nestor R
Robbins, Michael A
[et al.](#)

Publication Date

2019-11-01

DOI

10.1002/jor.24417

Peer reviewed



Published in final edited form as:

J Orthop Res. 2019 November ; 37(11): 2429–2436. doi:10.1002/jor.24417.

Acute Changes in NADPH Oxidase 4 in Early Post-Traumatic Osteoarthritis

Adam M. Wegner, M.D., Ph.D.^a, Nestor R. Campos, B.S.^a, Michael A. Robbins, M.D.^b, Andrew F. Haddad, B.S.^a, Hailey C. Cunningham, B.S.^a, Jasper H.N. Yik, Ph.D.^a, Blaine A. Christiansen, Ph.D.^a, Dominik R. Haudenschild, Ph.D.^a

^aUniversity of California Davis Medical Center, Sacramento, CA, 95817, USA

^bOregon Health & Science University, Department of Orthopaedics and Rehabilitation, Mail Code MP240, 3181 S.W. Sam Jackson Park Road, Portland, OR 97239, USA

Abstract

Knee injuries cause structural damage and acute inflammation that initiates the development of post-traumatic osteoarthritis (PTOA). NADPH oxidase 4 (Nox4), a member of a family of enzymes that generates reactive oxygen species (ROS), plays a pivotal role in normal development of the musculoskeletal system, but may increase ROS production to harmful levels after joint injury. The role of ROS in both normal joint homeostasis and injury is poorly understood, but inhibition of excessive ROS production by Nox4 after joint injury could be protective to the joint, decreasing oxidative stress and the initiation of PTOA. Knee injuries were simulated using inflammatory cytokines in cultured primary human chondrocytes and a non-invasive mouse model of PTOA in C57BL/6N and Nox4 knockout mice. There is an acute decrease in Nox4 activity within 24 hours after injury in both systems, followed by a subsequent sustained low-level increase, a novel finding not seen in any other system. Inhibition of Nox4 activity by GKT137831 was protective against early structural changes after non-invasive knee injury in a mouse model. Nox4 knockout mice had significant differences in structural and mechanical properties of bone, providing further evidence for the role of Nox4 in the development of joint tissues and biochemical response after joint injury. Nox4 plays a significant role in the acute phase after joint injury, and targeted inhibition of inflammation caused by Nox4 may be protective against early joint changes in the pathogenesis of PTOA.

Keywords

post-traumatic osteoarthritis; joint injury; antioxidant; inflammation; NADPH oxidase; Nox4

Address and all correspondence and reprint requests to: Dominik R. Haudenschild, Ph.D., UC Davis Medical Center, Department of Orthopaedic Surgery, 4635 2nd Avenue, Sacramento, CA 95817, Tel: (916) 734-5015, drhaudenschild@ucdavis.edu.

Contributions
All authors made substantial contributions to research design, acquisition of data, and analysis of data. They were all involved in drafting the paper or critically revising it, and all have read and approved the final submitted manuscript. Adam M. Wegner (adamwegner@gmail.com) and Dominik R. Haudenschild (drhaudenschild@ucdavis.edu) take responsibility for the integrity of the work as a whole, from inception to finished article.

Introduction

Osteoarthritis (OA) is a disease of the whole joint, affecting the functional unit of articular cartilage, subchondral bone, and synovium^{1; 2}. Post-traumatic osteoarthritis (PTOA), osteoarthritis that occurs after a joint injury such as an ACL tear, has an incidence of over 50% at 20 years after ACL tear and reconstruction^{3; 4}. While biomechanical stress on the joint is well accepted as an etiologic factor in the development of PTOA⁵, the cell signaling and biochemical factors involved in its pathogenesis are less appreciated. The initial inflammatory response after injury, generally thought to be important for healing in the body⁶, may also be harmful to the long-term health of articular cartilage and subchondral bone.

One potential component of the biochemical inflammatory response to joint injury is aberrant overproduction of reactive oxygen species (ROS). At low baseline levels, ROS are a component of cell signaling cascades in normal development and homeostasis of multiple body systems⁷, including tissues of the joint like cartilage and bone⁸. In the inflammatory response, overproduction of ROS is potentially harmful to tissues and may sensitize the joint to the development of post-traumatic osteoarthritis. It might follow that inhibition of post injury inflammation may protect body tissues from injury. However, results from high quality studies investigating non-specific antioxidants as treatments for various diseases caused by ROS overproduction have been inconsistent (For review, see⁹), most likely due to off target effects and concomitant inhibition of normal ROS signaling. Therefore, temporally and spatially targeted specific inhibition of aberrant ROS signaling in the inflammatory response after joint injury may have the potential to protect normal joint tissues and decrease early changes associated with the development of post-traumatic osteoarthritis without disrupting normal ROS signaling.

A source of ROS is NADPH Oxidase (Nox) 4, a member of the Nox family of proteins, the only protein family whose sole function is production of ROS¹⁰⁻¹². Elucidating the role of Nox4 in the acute inflammatory response after joint injury may provide insight into the molecular mechanisms behind the development of post-traumatic osteoarthritis, and inhibition of this response is a possible therapeutic target that may decrease the subsequent risk of PTOA. Nox4 constitutively produces hydrogen peroxide (H₂O₂)¹³ and is involved in the development and homeostasis of the tissues that compose the normal joint⁸. However, the effects of excess production of H₂O₂ by Nox4 in the context of joint pathology are unknown. It is upregulated in human diseases such as diabetes^{14; 15}, idiopathic pulmonary fibrosis¹⁶, and inflammatory brain diseases¹⁷, and the increase in Nox4 activity in diabetes is the target of a currently active phase II clinical trial of a Nox inhibitor, GKT137831¹⁸. This specific Nox1 and Nox4 inhibitor has a K_i from 100–150 nM in cell free assays¹⁹, does not inhibit other isoforms of Nox, xanthine oxidase, or the neutrophil oxidative burst, does not scavenge ROS, and has been previously shown to reverse fibrosis and improve survival in a mouse model of idiopathic pulmonary fibrosis^{20; 21}. Nox4 is also a potential therapeutic target in pre-clinical models of disease in many other systems including liver, kidney, brain, bone, skin, cardiovascular system, GI tract, and eye, and several forms of cancer²².

We hypothesized that excess production of H₂O₂ by Nox4 in the inflammatory response after joint injury is detrimental to tissues of the joint and that inhibition of this excess production would be protective. First, we characterized the production of H₂O₂ by Nox4 after joint injury *in vitro* in primary human chondrocytes, and *in vivo* in a non-invasive tibial compression mouse model of post-traumatic osteoarthritis. Second, we determined if inhibition of Nox4 after injury by GKT137831 is protective to the joint. Third, we characterized changes in the musculoskeletal system of Nox4 knockout mice, in relation to the role of Nox4 in acute structural changes of early PTOA. We observed acute changes in Nox4 expression and activity, supporting a role for Nox4 in the early stages of post-traumatic OA.

Methods

Human articular chondrocyte culture

Human articular chondrocytes were obtained from young healthy males and females (ages 13–48) undergoing arthroscopic ACL reconstruction (with Institutional Review Board approval and patient consent). Isolation and monolayer culture of human articular chondrocytes was modified from a method described by Barbero and Martin designed to minimize de-differentiation during passage²³. Harvested chondrocytes were digested overnight in 0.15% collagenase (Sigma-Aldrich, St. Louis, MO, USA), plated at 10,000 cells/cm², and cultured in chondrocyte media: Dulbecco's Modified Eagle's medium (DMEM) supplemented with 10 mM HEPES buffer, 1% Penicillin/Streptomycin, MEM Non-Essential Amino acids, 10% fetal bovine serum (FBS), all from Gibco/Life Technologies/ThermoFisher Scientific (Grand Island, NY, USA), and 5 ng/ml FGF (R&D Systems, Minneapolis, MN, USA). For experiments, 500,000 chondrocytes that were at passage 4 or below were seeded per well in a 12 well dish, and treated with various drugs in the above DMEM media without FBS or FGF added: 1mM GKT137831 (a gift from Genkyotex S. A., Geneva, Switzerland, dissolved in 1.2 wt% methylcellulose + 0.1% wt% Polysorbate 90 in water)²¹ or cytokines 10 ng/ml of IL-1 β , TNF- α , or TGF- β (R&D Systems). All chondrocyte experiments were repeated in triplicate and reported as the mean \pm standard deviation.

Hydrogen peroxide assay

500,000 human articular chondrocytes were plated in 12 well dishes and serum starved overnight in chondrocyte media with 0.1% FBS. Media was changed to serum free chondrocyte media without Phenol Red for experiments. Cells were treated with cytokines or drugs for specified periods of time. Assays were performed based on the manufacturer's instructions from the Amplex Red Hydrogen Peroxide/Peroxidase Assay Kit (Life Technologies/ThermoFisher Scientific, Waltham, MA, USA). Briefly, Amplex Red was added to the media for the last 45 minutes of treatment. 150 μ l was transferred to one well of a black 96 well plate in duplicate and read on FilterMax F5 Multi-Mode Microplate Reader (Molecular Devices, Sunnyvale, CA, USA) at an excitation of 535 nm and emission of 590 nm. Each experiment was performed in at least 4 different chondrocyte lines to account for variability between human tissue donors. A standard curve was used in each experiment to verify that the readings were in the linear range of the assay and relative

fluorescence unit (RFU) measurements were converted to H₂O₂ concentrations (nM to single digit μ M range). Values were expressed as % change to allow for normalization across experiments.

Tibial compression induced knee injury

Female wild-type (WT) C57BL/6N mice and Nox4 knockout (KO) mice (B.6129-Nox4^{tm1Kkr}/J) were obtained from Jackson Labs (Bar Harbor, ME, USA). Female mice were used for experiments to eliminate added activity from male fighting and to eliminate the effects of isolating aggressive animals to individual housing. Animals were maintained and used per the National Institutes of Health Guidelines on the Care and Use of Laboratory Animals and all protocols were approved by the University of California Davis Institutional Animal Care and Use Committee (IACUC). Nox4 knockout mice were genotyped and bred by the University of California, Davis, Mouse Biology Program (MBP).

Animals were kept in a housing facility for a 2-week acclimation period before non-invasive mouse knee joint injury was performed at 10 weeks of age as previously described^{24; 25}. Briefly, the right knees of the mice were injured in a single dynamic overload at 1 mm/s to a target compressive force of 14 N using an electromagnetic material testing system (ELF 3200, Bose, Eden Prairie, MN, USA). This rate of loading has previously been shown by our group to reliably cause a bony avulsion of the ACL off of the tibia.²⁵ The load was manually stopped immediately after rupture of the ACL occurred, which was determined by audible click from the knee as well as release of compressive force on the testing system readout.

Pharmacological Inhibition of Nox4

Mice that received GKT137831 were given 20 mg/ml daily through gavage starting on day 0 immediately after injury through day 7 when the animals were sacrificed. Control animals were given gavage of an equal volume of vehicle (1.2% w/v methylcellulose and 0.1% w/v Polysorbate 80 prepared in water).

RNA isolation and gene expression analysis

Mice (n=80 total) were euthanized 2, 4, 6, 8, 18, 24, 48, 72, 96, and 168 hours after injury with CO₂ per IACUC-approved protocol, and injured right knees and control left knees were micro-dissected while submerged under RNALater (Qiagen, Valencia, CA, USA) to strip muscle down to the knee joint capsule. Bone was cut at the femoral and tibial epiphyses. The joint was snap-frozen in liquid N₂, and ground in a mortar and pestle under liquid nitrogen. Liquid N₂ was evaporated at -80°C, and the homogenized joint powder dissolved in 1.5 ml Qiazol (Qiagen).

RNA was isolated from human chondrocytes or homogenized mouse knees using the same protocol. Qiazol was added to chondrocytes in a 12 well dish (700 μ l) or knee homogenates (1.5 ml) and agitated with a pipette. The mixture was then run through a QiaShredder column (Qiagen) and RNA was then purified using a miRNeasy kit (Qiagen) according to provided instructions. The flow-through from the miRNeasy columns was stored at -80C for subsequent protein isolation.

cDNA was generated by reverse transcription using the QuantiTect Reverse Transcription kit (Qiagen). 2 µl of cDNA and 5 µl of MasterMix were used in a final volume of 10 µl. Samples were run in triplicate on a 7900HT RT-PCR system (Applied Biosystems, Foster City, CA, USA). PrimeTime® Std qPCR Assay probes were from Integrate DNA Technologies (IDT, Coralville, IA, USA) as follows: Human Nox4 assays Hs.PT.58.22926436 and HS.PT.58.3866448, Mouse Nox4 assays Mm.PT.58.8820983 and Mm.PT.58.161191131. All samples were normalized using 18S ribosome control primer from Applied Biosystems (Foster City, CA). Probes were used per manufacturer's instructions. mRNA was quantified using the 2^{-Ct} method²⁶.

Protein purification and western blotting

Protein was isolated from flow-through of the RNA isolation protocol, as recommended by Qiagen. Briefly, ethanol was added to the pink organic layer of Qiazol lysate from chondrocytes or whole mouse knees, after chloroform extraction was performed, to precipitate out DNA, then isopropanol was added to precipitate protein. The protein pellet was washed 2 times with 1ml 0.3 M guanidine hydrochloride in 95% EtOH, then re-suspended in 2 M urea and 1% SDS in PBS. Protein was normalized using the Pierce BCA Protein Assay Kit (Thermo Scientific, Rockland, IL, USA) and lanes loaded with equal amounts of protein in sample loading buffer (50 mM Tris HCl, pH 6.8, 100 mM dithiothreitol, 4% 2-mercaptoethanol, 2% sodium dodecyl sulfate (SDS), and 10% glycerol). Protein was resolved on 4–12% SDS-polyacrylamide gels and transferred to Immobilon-P PVDF membrane (EMD Millipore, Billerica, MA, USA). Membranes were blocked for 1 hour with 3% skim milk in TBST (25 mM Tris HCl, pH 7.5, 125 mM NaCl; 0.1% Tween 20), followed by overnight incubation at 4°C with Nox4 antibody (Novus, Littleton, CO, USA). Blots were probed with anti-rabbit horseradish peroxidase (HRP) conjugated secondary (PerkinElmer Inc., Waltham, MA, USA) for 1 hour, then visualized with an Alpha Innotec FluorChem Digital Imaging System. To normalize loading, blots were then stripped with 0.2M NaOH at RT for 5 min, re-blocked with 3% milk, and incubated overnight at 4°C with β-actin antibody (Santa Cruz Biotechnology, Dallas, TX, USA), probed with anti-mouse HRP conjugated secondary, and visualized.

µCT Bone Analysis

Femurs and tibias from uninjured 10-week old WT (n=5) and Nox-4 KO (n=5) mice were measured with a micrometer to determine bone length. Bilateral knees of injured mice (n=6/group) were harvested, fixed at a 90-degree angle per the protocol described in Dymont et al. using pins, fixed in 4% paraformaldehyde overnight at 4°C, then preserved at 4°C in 70% ethanol²⁷. Femurs from uninjured mice were imaged with micro-computed tomography (SCANCO µCT35, Brüttisellen, Switzerland) to quantify trabecular bone structure in the distal femoral epiphysis and metaphysis, and cortical bone structure at the mid-diaphysis. Knees from injured mice were imaged to quantify trabecular bone microstructure of the distal femoral epiphysis. Settings for µCT analysis of rodent bone were as follows: x-ray tube potential = 55 kVp, current = 114 µA, integration time = 900 ms, number of projections = 1000/180°, with isotropic nominal voxel sizes of 6 µM for uninjured bones and 10 µM for injured knees²⁸.

Data were analyzed as described previously²⁴. Briefly, trabecular bone was analyzed by manually drawing contours on 2D transverse slices. The distal femoral epiphysis was designated as the region of trabecular bone enclosed by the growth plate and subchondral cortical bone plate. The distal femoral metaphysis was designated as the region of trabecular bone immediately adjacent to the distal growth plate, extending 150 slices (900 μm) proximal. We quantified trabecular bone volume fraction (BV/TV), trabecular thickness (Tb.Th), trabecular number (Tb.N), apparent bone mineral density (Apparent vBMD; mg HA/cm³ TV), and other structural outcomes using the manufacturer's analysis tools. Cortical bone was analyzed using a 100 slice (600 μm) volume of interest centered at the midpoint of the diaphysis. We quantified bending moments of inertia (I_{max} and I_{min}), bone area (B.Ar), total cross-sectional area (T.Ar), cortical thickness (C.Th), and tissue mineral density (vTMD; mg HA/cm³ BV) using the manufacturer's analysis tools.

Three-Point Bending

Following μCT scanning, femurs were rehydrated for 10–15 minutes in phosphate buffered saline (PBS), then mechanically tested in three-point bending with the anterior surface of the bone in tension to determine cortical bone material properties. The lower supports had a span of 7.45 mm, and the center loading platen was driven at 0.1 mm/sec until failure. Resulting force and displacement data were analyzed to determine stiffness and ultimate force. Modulus of elasticity and ultimate stress were determined using Euler-Bernoulli beam theory.

Statistics

Student's t-test was used to compare levels of H₂O₂, protein, and mRNA in primary human chondrocytes, μCT data, and Nox4 protein levels. In Figure 2, two methods were used to determine significance: Method 1: At each time point, the two-sided t-test was used to test $H_0: \mu = 0$ versus $H_a: \mu \neq 0$. Method 2: We fit a linear model to the entire data set in which we created nine design variables for the ten time courses with 2 hours as a referent to estimate the expected delta Ct with respect to the contralateral knee of the same animal to construct 95% confidence intervals of the expected fold change and used a two-sided t-test to test $H_0: \mu = 0$ versus $H_a: \mu \neq 0$ with 72 degrees of freedom (Number of data at all time points – 10 = 82 – 10 = 72). All analyses were performed with SAS version 9.4 (SAS Institute Inc., Cary, NC, USA). In Figure 3, one-way ANOVA with post-hoc Tukey HSD test was used to ascertain differences between baseline BV/TV and differences before and after injury. p-value < 0.05 was considered statistically significant in all tests.

Results

Articular Chondrocyte Assays

Production of hydrogen peroxide by Nox4 is hypothesized to be a component of the inflammatory response to injury, but the kinetics of Nox4 activation after joint injury remain unknown. A simulated joint injury was performed on cultured primary human chondrocytes through treatment with catabolic cytokines (IL-1 β or TNF- α). We consistently observed an acute initial decrease in H₂O₂ production, Nox4 mRNA expression, and Nox4 protein expression immediately after treatment with either IL-1 β or TNF- α (Fig. 1A, 1B).

Treatment with an anabolic cytokine (TGF- β) has the opposite effect acutely on H₂O₂ production and Nox4 mRNA and protein levels (Fig. 1C). The increase in H₂O₂ production elicited by TGF- β was inhibited by the Nox1/4 specific inhibitor GKT137831 (Fig. 1D). H₂O₂ production was in the micromolar range.

Mouse Knee Injury Results

Early changes in Nox4 were studied in a mouse model of joint injury, in which a single tibial compression causes ACL-rupture and consistently leads to PTOA within a 4–8 week timespan. This non-invasive model is advantageous because it allows for assessment of acute biochemical changes in the joint immediately after injury. The uninjured contralateral left knees served as a control for injured right knees and were used to normalize Nox4 mRNA or protein levels. A significant decrease in Nox4 mRNA was seen as early as two hours after joint injury (Fig. 2A). This decrease was sustained up to 24 hours, after which Nox4 expression increased above the pre-injury levels. A peak in Nox4 mRNA levels was observed at 48 hours ($p < 0.05$), and Nox4 mRNA levels remained significantly elevated out to 72 hours post-injury ($p < 0.05$), and slightly elevated out to 4 and 7 days. A similar trend was seen with Nox4 protein levels (Fig. 2B).

μ CT Results

Since we observed this sustained low level of increased Nox4 expression during the first 2–7 days after injury, we next examined whether a lack of Nox4 activity in Nox4 KO mice or a Nox4 inhibitor (GKT137831) in WT mice would affect the injury-induced changes in joint structures. We treated C57Bl/6 mice with vehicle or a Nox4 inhibitor (GKT137831) daily by gavage after joint injury. Subchondral bone was examined by high-resolution μ CT at 7-days post-injury, a time point where maximal changes in subchondral bone density (BV/TV) were previously observed²⁴. A decrease in subchondral bone density is one of the early acute structural changes of the joint that may lead to eventual PTOA. The mean baseline BV/TV in Nox4 KO mice (0.28) was significantly less than in WT mice (0.32) and WT mice treated with Nox4 inhibitor for 7 days (0.33) (Fig. 3). Wild-type mice treated with vehicle (0.07) and Nox4 KO mice (0.08) had a statistically significant decrease in subchondral bone density (BV/TV), while injured knees from Wild-type mice treated with Nox4 inhibitor did not (0.04) (Fig. 3).

In order to determine the effect of a lack of Nox4 activity on the homeostasis of bone and how that might elucidate the role of Nox4 in early structural changes to the joint after injury, we performed a characterization and comparison of structural and mechanical properties of bones from WT and Nox4 KO mice. The KO mice had no gross phenotype, which is in accordance with previous studies²⁹. KO mice had significantly decreased epiphyseal and metaphyseal BV/TV and trabecular number, with increased trabecular thickness in the epiphysis, and increased Tissue Mineral Density (TMD) in the mid-diaphysis (Fig. 4), all indicating changes in bone quality of the Nox4 knockout mice.

Mechanical Testing Results

In mechanical testing, bone from Nox4 knockout mice was stiffer than bone from WT mice, with no difference in ultimate force, modulus, or ultimate stress (Fig. 5). The femurs of WT

mice (14.47 ± 0.31) are slightly shorter than those of Nox4 KO mice (14.93 ± 0.51), but there was no difference in tibial length (17.78 ± 1.63 vs. 17.99 ± 0.96).

Discussion

The first goal of this study was to use *in vitro* human and *in vivo* mouse models to characterize the role of Nox4 and H₂O₂ in the early inflammatory response to joint injury. We hypothesized that Nox4 would produce an excessive amount of H₂O₂ in the initial inflammatory phase, that this excessive H₂O₂ production may lead to initiation of changes consistent with post-traumatic osteoarthritis, and that targeted inhibition of this initial inflammatory response may be protective. We observed an unexpected initial decrease in Nox4 protein and activity in the first 48 hours followed by a sustained increase that was observed in both *in vivo* mouse knees and *in vitro* human chondrocytes.

Although the initial decreases in Nox4 activity, mRNA, and protein were not predicted by results from other systems^{14–17}, these results were reproducible and consistent between *in vitro* and *in vivo* experiments. We also observed an overall consistency between Nox4 enzymatic functional assays and its mRNA and protein levels, which was expected since Nox4 is constitutively active³⁰. The non-invasive aspect of the murine tibial compression induced post-traumatic osteoarthritis model allows for assessment of the early acute time points *in vivo* required to observe this initial decrease. This model also allows for study of the entire knee joint between the subchondral bone of the distal femur to the subchondral bone of the proximal tibia. The *in vitro* studies used primary human chondrocytes, a unique model that allows for the closest approximation to the human condition without obtaining actual injured human knee joints.

The second goal of the study was to determine if inhibition of Nox4 after injury was protective to the joint. Inhibition of Nox4 after injury *in vitro* abrogated the excess production of H₂O₂ and *in vivo* it attenuated an early decrease in subchondral bone density, suggesting that it may be protective against early changes in the development of post-traumatic osteoarthritis. Finally, characterization of a Nox4 knockout mouse indicated significant effects of a lack of Nox4 on bone structure, providing further evidence for a possible role of Nox4 in the pathogenesis of PTOA.

One limitation of this study is that it was focused on the acute changes after knee joint injury. Time points longer than several days in chondrocytes and time points longer than one week in mice were not obtained. Due to temporal limitations in the health of the primary human chondrocyte, longer *in vitro* time points may not be feasible. Future studies may be performed in mice to observe the longer-term biochemical and structural effects of joint injury and inhibition of Nox4. Another limitation of the study is the inability to perform functional Nox4 assays in whole joint tissue. It is also not possible to obtain whole human knees, so the mouse model must be used as a surrogate. The limitation of the mouse Nox4 knockout is that there is no tissue specific or temporal specific knockout. There is also the potential for compensation or redundancy in the Nox4 system, and although we did not investigate that possibility in the current study, several previous studies demonstrate that there are no compensatory changes in other Nox family members however^{31; 32}. Nox4 is

involved in osteoblastogenesis and osteoclastogenesis⁸, so the effect of a lack of Nox4 activity on bone development vs. homeostasis was not able to be ascertained in this study. Therefore, the etiology of decreased baseline BV/TV and susceptibility of BV/TV to joint injury in the Nox4 KO versus wild-type is unknown. Other joint tissues such as articular cartilage and synovium were also not studied. Finally, only female mice were used in the study, so the broad applicability to males is unknown and further study of both sexes may further clarify the role of Nox4 in bone development and maintenance and post-traumatic osteoarthritis.

There are two previous reports of a potential role for Nox4 in osteoarthritis. IL-1B stimulation in an immortalized human chondrocyte cell line (C-20/A4 cells) overexpressing Nox4 generated increased H₂O₂ production and matrix metalloproteinase activity (MMP1) compared to normal cells³³. Our results corroborate and extend this study in a more physiological system without overexpression of Nox4 and in both murine and human models. A second study in primary human articular chondrocytes from femoral heads found that 24h of IL-1B stimulation increased production of H₂O₂³⁴. This is in contrast to decreased in Nox4 activity, mRNA, and protein observed here at 24h. The difference may potentially be explained by the fact that chondrocytes from this study are from knees rather than femoral heads. Our results were consistent across H₂O₂ production, Nox4 mRNA levels, and Nox4 protein levels, as well as our in vivo experiments in mice. Further work will be needed to reconcile the discrepancy between these two reports.

In the musculoskeletal system, Nox4 has been studied as a drug target in several preclinical models of osteoporosis²². Goettsch et al. found that the distal femur of Nox4 knockout mice had higher trabecular bone density, weight, and thickness, similar trabecular number and separation, and reduced osteoclasts³⁵. This is in contrast to our study of the epiphyseal bone of Nox4 knockout mice, where we found decreased bone density and quality in Nox4 KO mice. The mice used in the previous study are of unknown age, whereas the mice in this study were young (10 wks). This young age was chosen because knee injuries that lead to post-traumatic arthritis often occur at a relatively young age, and 10 weeks of age in mice is approximately equivalent to a young adult. Further studies should investigate the effect of Nox4 knockout as well as the effect of knee injury in all ages of mice. Our measurements were also obtained using μ CT and limited to the epiphysis, which may be more relevant to changes in post-traumatic osteoarthritis, whereas the measurements in the previous study were from histomorphometry and taken of the entire distal femur.

The decrease in subchondral bone density in post-traumatic osteoarthritis has been a therapeutic target in several preclinical studies in rabbits. This is a natural extension of work implicating Nox4 in osteoporosis⁸. These studies provide an important first step in understanding changes after knee injury that may lead to PTOA, but this single parameter of a decrease in subchondral bone density is one small aspect of the whole joint inflammatory response. Inhibition of this inflammatory response, such as production of free radicals by Nox4 that results in a decrease in subchondral bone density, among other detrimental changes, may more broadly decrease the early changes of PTOA, although further study is warranted.

Acknowledgments

Salary (A.M.W) and research funding to support this project was generously provided by a gift of Denny and Jeanene Dickenson. This project was also supported by a Resident Clinician Scientist Training Grant (14–025) from the Orthopaedic Research and Education Foundation (OREF), with funding provided by the Ira A. Rochelle Family foundation, to A.M.W and an Orthopaedic Trauma Association (OTA) Grant to A.M.W. Portions of the project described was supported by the National Center for Advancing Translational Sciences (NCATS), National Institutes of Health (NIH), through grant #UL1 TR000002. GKT137831 was generously provided by Genkyotex. We are grateful for the technical support, products, and services provided to our research by the Mouse Biology Program (www.mousebiology.org) at the University of California, Davis.

None of the authors have any conflicts of interest with this study, including through employment, consultancies, stock ownership, honoraria, paid expert testimony, patent applications/registrations, research grants, or other funding.

References

1. Di Cesare PE, Haudenschild DR, Samuels J, et al. 2013 Pathogenesis of Osteoarthritis In: Firestein GS, Kelley WN editors. Kelley's Textbook of Rheumatology, 9th ed; pp. 1617–1635.
2. Lories RJ, Luyten FP. 2011 The bone-cartilage unit in osteoarthritis. *Nature reviews Rheumatology* 7:43–49. [PubMed: 21135881]
3. Cinque ME, Dornan GJ, Chahla J, et al. 2017 High Rates of Osteoarthritis Develop After Anterior Cruciate Ligament Surgery: An Analysis of 4108 Patients. *The American journal of sports medicine*:363546517730072.
4. Lohmander LS, Englund PM, Dahl LL, et al. 2007 The long-term consequence of anterior cruciate ligament and meniscus injuries: osteoarthritis. *The American journal of sports medicine* 35:1756–1769. [PubMed: 17761605]
5. Martin JA, Anderson DD, Goetz JE, et al. 2017 Complementary models reveal cellular responses to contact stresses that contribute to post-traumatic osteoarthritis. *J Orthop Res* 35:515–523. [PubMed: 27509320]
6. Anderson DD, Chubinskaya S, Guilak F, et al. 2011 Post-traumatic osteoarthritis: improved understanding and opportunities for early intervention. *J Orthop Res* 29:802–809. [PubMed: 21520254]
7. Di Meo S, Reed TT, Venditti P, et al. 2016 Role of ROS and RNS Sources in Physiological and Pathological Conditions. *Oxid Med Cell Longev* 2016:1245049. [PubMed: 27478531]
8. Schroder K 2014 NADPH oxidases in bone homeostasis and osteoporosis. *Cellular and molecular life sciences* : CMLS.
9. Hajhashemi V, Vaseghi G, Pourfarzam M, et al. 2010 Are antioxidants helpful for disease prevention? *Res Pharm Sci* 5:1–8. [PubMed: 21589762]
10. Sumimoto H 2008 Structure, regulation and evolution of Nox-family NADPH oxidases that produce reactive oxygen species. *FEBS J* 275:3249–3277. [PubMed: 18513324]
11. Altenhofer S, Kleikers PW, Radermacher KA, et al. 2012 The NOX toolbox: validating the role of NADPH oxidases in physiology and disease. *Cellular and molecular life sciences* : CMLS 69:2327–2343. [PubMed: 22648375]
12. Bedard K, Krause KH. 2007 The NOX family of ROS-generating NADPH oxidases: physiology and pathophysiology. *Physiol Rev* 87:245–313. [PubMed: 17237347]
13. Nisimoto Y, Diebold BA, Cosentino-Gomes D, et al. 2014 Nox4: a hydrogen peroxide-generating oxygen sensor. *Biochemistry* 53:5111–5120. [PubMed: 25062272]
14. Gorin Y, Block K, Hernandez J, et al. 2005 Nox4 NAD(P)H oxidase mediates hypertrophy and fibronectin expression in the diabetic kidney. *The Journal of biological chemistry* 280:39616–39626. [PubMed: 16135519]
15. Sedek M, Callera G, Montezano A, et al. 2010 Critical role of Nox4-based NADPH oxidase in glucose-induced oxidative stress in the kidney: implications in type 2 diabetic nephropathy. *Am J Physiol Renal Physiol* 299:F1348–1358. [PubMed: 20630933]

16. Amara N, Goven D, Prost F, et al. 2010 NOX4/NADPH oxidase expression is increased in pulmonary fibroblasts from patients with idiopathic pulmonary fibrosis and mediates TGFbeta1-induced fibroblast differentiation into myofibroblasts. *Thorax* 65:733–738. [PubMed: 20685750]
17. Basuroy S, Bhattacharya S, Leffler CW, et al. 2009 Nox4 NADPH oxidase mediates oxidative stress and apoptosis caused by TNF-alpha in cerebral vascular endothelial cells. *Am J Physiol Cell Physiol* 296:C422–432. [PubMed: 19118162]
18. SAS GI. Safety and Efficacy of Oral GKT137831 in Patient With Type 2 Diabetes and Albuminuria [ClinicalTrials.gov identifier NCT02010242] US National Institutes of Health, ClinicalTrials.gov [online]. Available from URL: <https://clinicaltrials.gov> [Accessed 2016 2 21].
19. Jiang JX, Chen X, Serizawa N, et al. 2012 Liver fibrosis and hepatocyte apoptosis are attenuated by GKT137831, a novel NOX4/NOX1 inhibitor in vivo. *Free radical biology & medicine* 53:289–296. [PubMed: 22618020]
20. Hecker L, Logsdon NJ, Kurundkar D, et al. 2014 Reversal of persistent fibrosis in aging by targeting Nox4-Nrf2 redox imbalance. *Sci Transl Med* 6:231ra247.
21. Laleu B, Gaggini F, Orchard M, et al. 2010 First in class, potent, and orally bioavailable NADPH oxidase isoform 4 (Nox4) inhibitors for the treatment of idiopathic pulmonary fibrosis. *J Med Chem* 53:7715–7730. [PubMed: 20942471]
22. Teixeira G, Szyndralewicz C, Molango S, et al. 2017 Therapeutic potential of NADPH oxidase 1/4 inhibitors. *British journal of pharmacology* 174:1647–1669. [PubMed: 27273790]
23. Barbero A, Martin I. 2007 Human articular chondrocytes culture. *Methods Mol Med* 140:237–247. [PubMed: 18085212]
24. Christiansen BA, Anderson MJ, Lee CA, et al. 2012 Musculoskeletal changes following non-invasive knee injury using a novel mouse model of post-traumatic osteoarthritis. *Osteoarthritis Cartilage* 20:773–782. [PubMed: 22531459]
25. Lockwood KA, Chu BT, Anderson MJ, et al. 2014 Comparison of loading rate-dependent injury modes in a murine model of post-traumatic osteoarthritis. *J Orthop Res* 32:79–88. [PubMed: 24019199]
26. Livak KJ, Schmittgen TD. 2001 Analysis of relative gene expression data using real-time quantitative PCR and the 2(-Delta Delta C(T)) Method. *Methods* 25:402–408. [PubMed: 11846609]
27. Dymant NA, Hagiwara Y, Jiang X, et al. 2015 Response of knee fibrocartilage to joint destabilization. *Osteoarthritis Cartilage* 23:996–1006. [PubMed: 25680653]
28. Bouxsein ML, Boyd SK, Christiansen BA, et al. 2010 Guidelines for assessment of bone microstructure in rodents using micro-computed tomography. *Journal of bone and mineral research : the official journal of the American Society for Bone and Mineral Research* 25:1468–1486.
29. Sirokmany G, Donko A, Geiszt M. 2016 Nox/Duox Family of NADPH Oxidases: Lessons from Knockout Mouse Models. *Trends Pharmacol Sci* 37:318–327. [PubMed: 26861575]
30. Serrander L, Cartier L, Bedard K, et al. 2007 NOX4 activity is determined by mRNA levels and reveals a unique pattern of ROS generation. *The Biochemical journal* 406:105–114. [PubMed: 17501721]
31. Kleinschnitz C, Grund H, Wingler K, et al. 2010 Post-stroke inhibition of induced NADPH oxidase type 4 prevents oxidative stress and neurodegeneration. *PLoS Biol* 8.
32. Zhang M, Brewer AC, Schroder K, et al. 2010 NADPH oxidase-4 mediates protection against chronic load-induced stress in mouse hearts by enhancing angiogenesis. *Proceedings of the National Academy of Sciences of the United States of America* 107:18121–18126. [PubMed: 20921387]
33. Grange L, Nguyen MV, Lardy B, et al. 2006 NAD(P)H oxidase activity of Nox4 in chondrocytes is both inducible and involved in collagenase expression. *Antioxidants & redox signaling* 8:1485–1496. [PubMed: 16987005]
34. Rousset F, Hazane-Puch F, Pinosa C, et al. 2015 IL-1beta mediates MMP secretion and IL-1beta neosynthesis via upregulation of p22(phox) and NOX4 activity in human articular chondrocytes. *Osteoarthritis Cartilage* 23:1972–1980. [PubMed: 26521743]

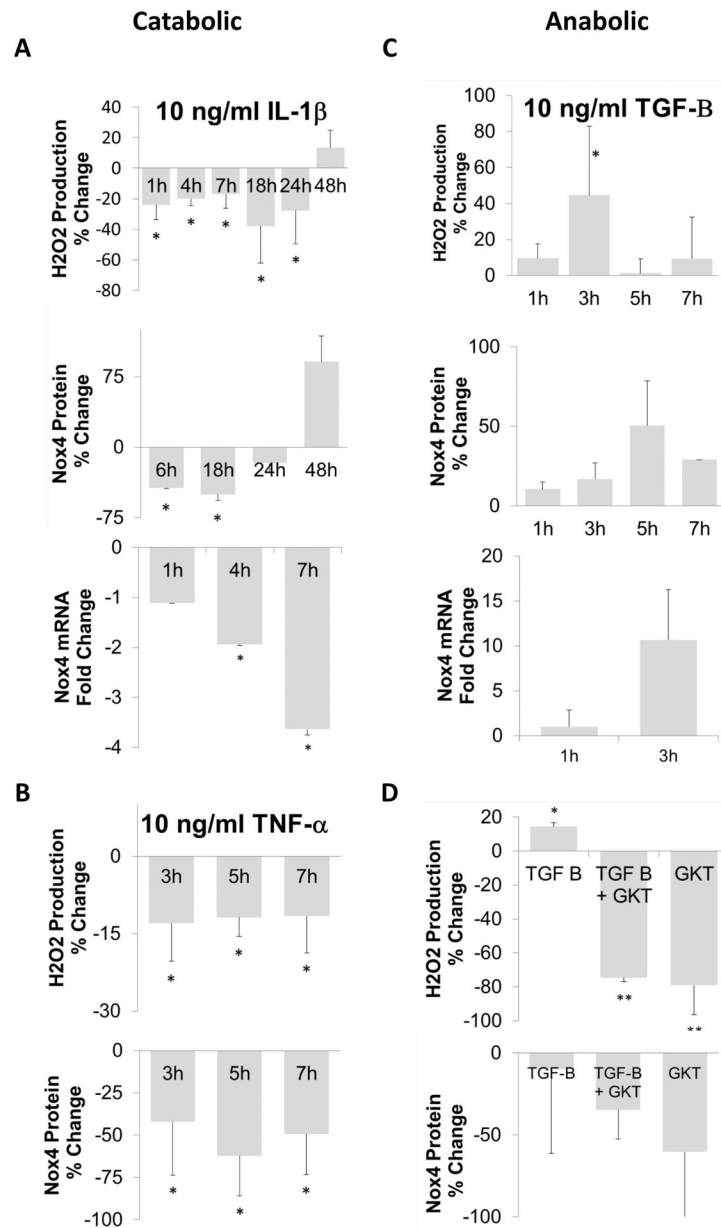
35. Goettsch C, Babelova A, Trummer O, et al. 2013 NADPH oxidase 4 limits bone mass by promoting osteoclastogenesis. *The Journal of clinical investigation* 123:4731–4738. [PubMed: 24216508]

Author Manuscript

Author Manuscript

Author Manuscript

Author Manuscript

**Figure 1.**

Nox4 activity, protein, and mRNA expression in primary human chondrocytes after cytokine treatment with or without Nox4 inhibition. Kinetics of hydrogen peroxide production (top), Nox4 protein (middle), and Nox4 mRNA expression (bottom) in response to catabolic cytokines: (A) 10 ng/ml IL-1 β treatment or (B) 10 ng/ml TNF- α treatment. (C) Kinetics of Nox4 activity and expression after addition of 10 ng/ml TGF- β , an anabolic cytokine. (D) Suppression of the TGF- β mediated increase in hydrogen peroxide production and Nox4 protein levels in response to TGF- β and TGF- β + 1 mM GKT137831 treatment. In all experiments, percent change from baseline H2O2 production was measured by Amplex Red Assay, fold change in mRNA expression was measured by quantitative reverse transcription-

polymerase chain reaction, and protein was measured by western blot and is in comparison to vehicle treated cells. * indicates $p < 0.05$ compared to vehicle treated control.

Author Manuscript

Author Manuscript

Author Manuscript

Author Manuscript

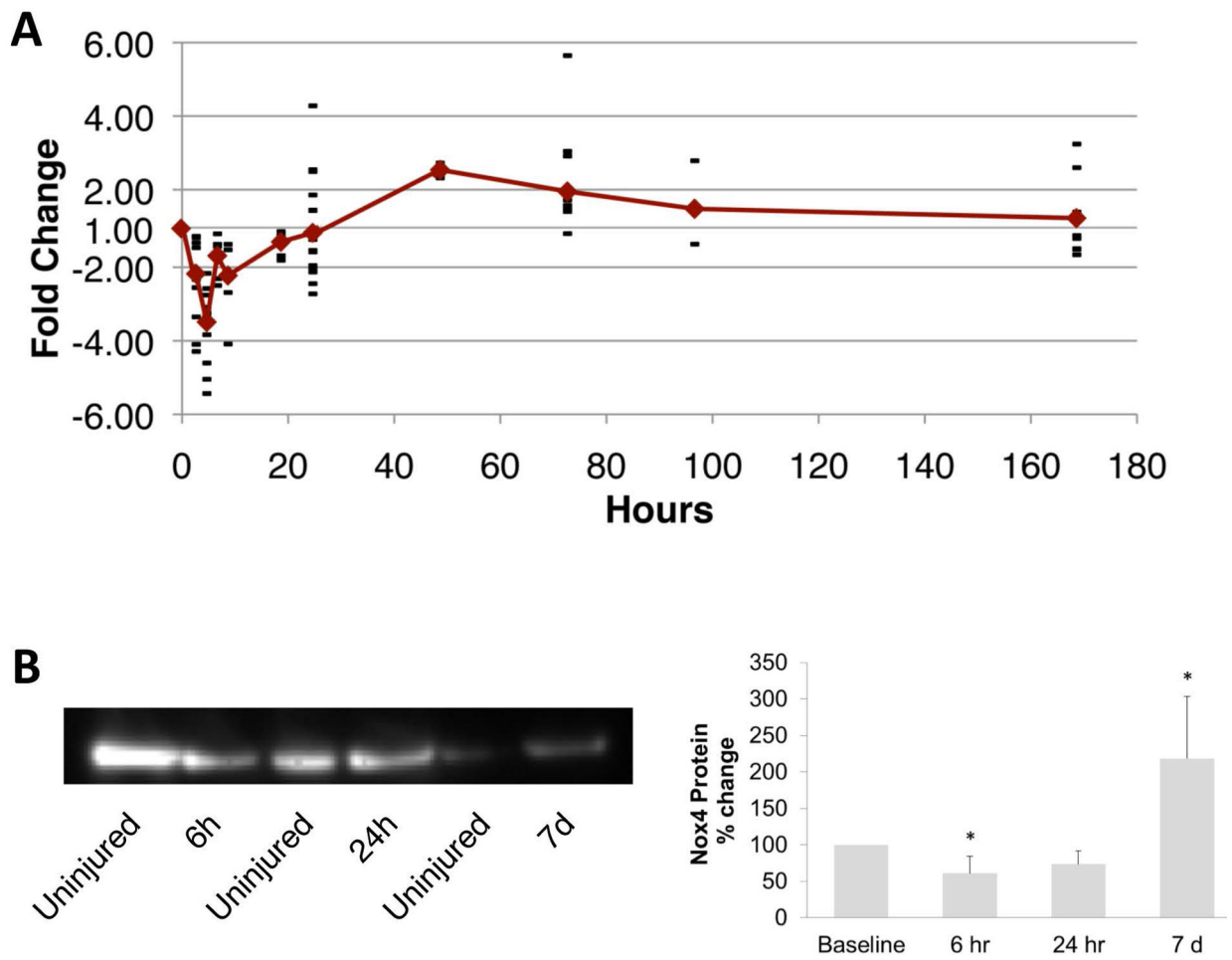


Figure 2.

Kinetics of Nox4 mRNA expression as measured by RT-PCR (A) and protein as measured by western blot (B) after non-invasive ACL rupture of right knees of 10-week old female C57Bl/6 mice compared to control left knees from the same animals. * indicates $p < 0.05$.

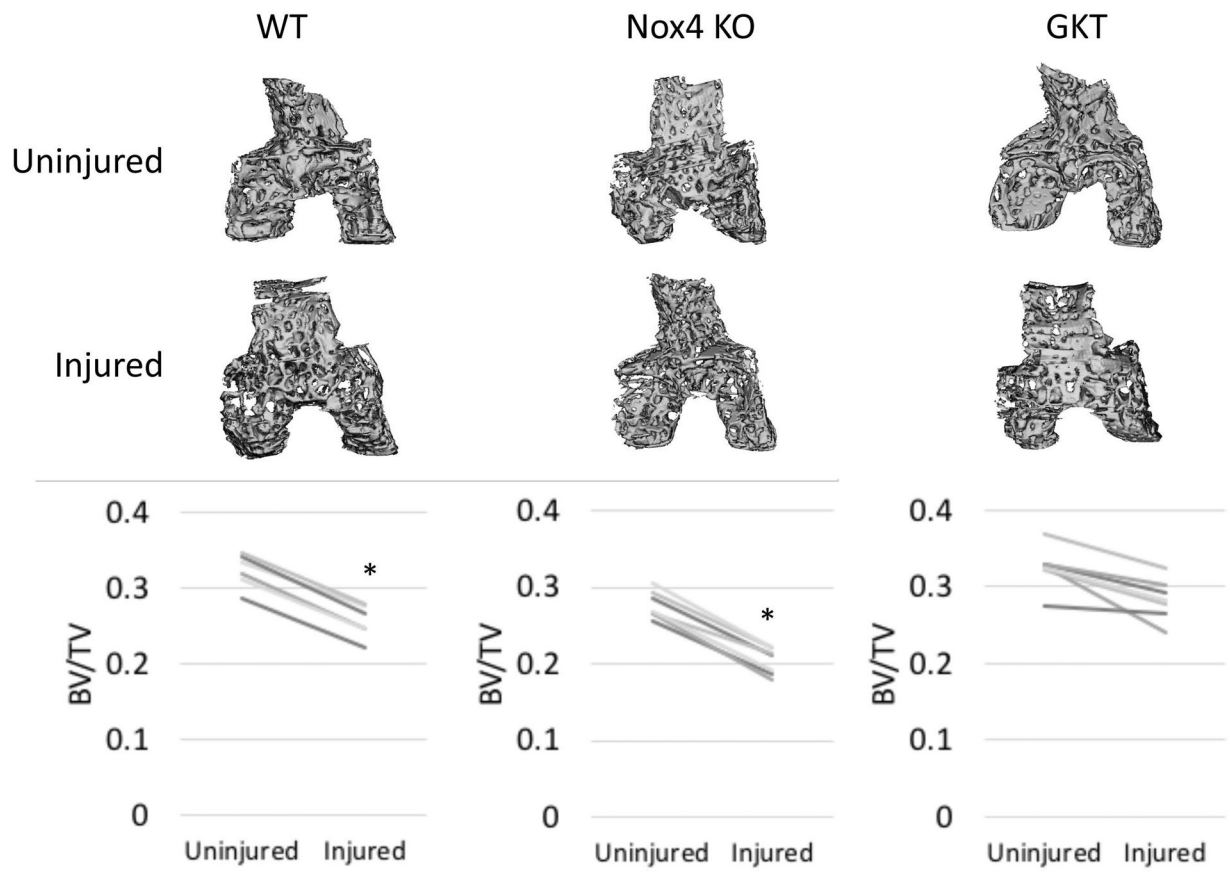


Figure 3. μ CT assessment of bone density (bone volume/total volume) 7 days after non-invasive joint injury in untreated wild-type mice, Nox4 knockout mice, and wild-type mice treated with the Nox4 inhibitor GKT137831. Mouse knee μ CT 3-D reconstructions (top) and graphs of BV/TV of left/right pairs of knees (bottom) from female B57Bl/6 mice 7 days after non-invasive knee injury. Mice were treated with either GKT137831 compound or vehicle by gavage on the day of injury and every day thereafter. n=7 per condition. * indicates p < 0.05.

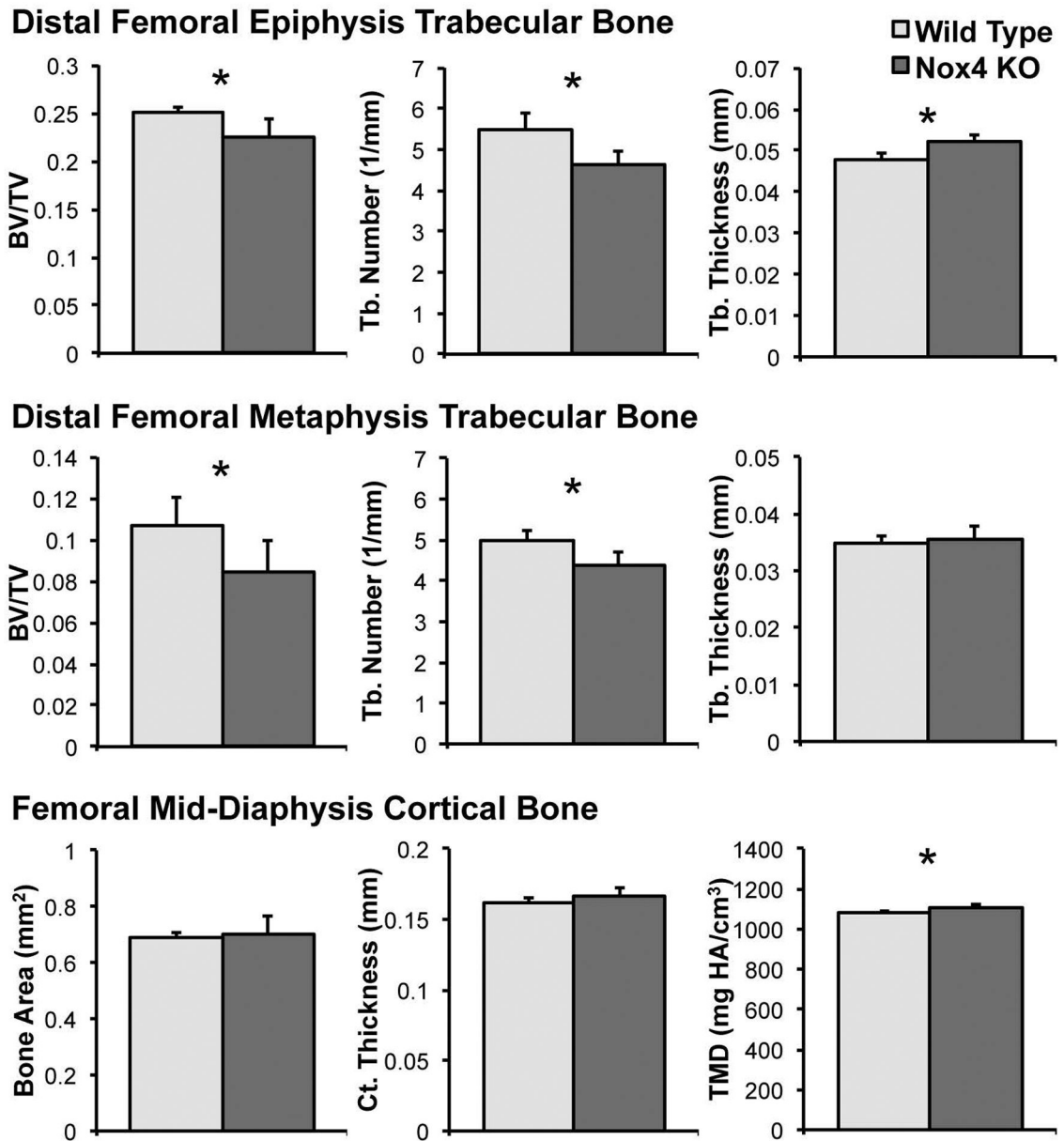


Figure 4.

μ CT analysis of young (10 week old) wild type vs. Nox4 knockout mice. Quantification of epiphyseal and metaphysis bone volume over total volume (BV/TV) and trabecular number (Tb. Number), epiphyseal trabecular thickness (Tb. Thickness), and mid-diaphyseal tissue mineral density (TMD) shows significant differences in the knockout mice for all characteristics. * indicates $p < 0.05$.

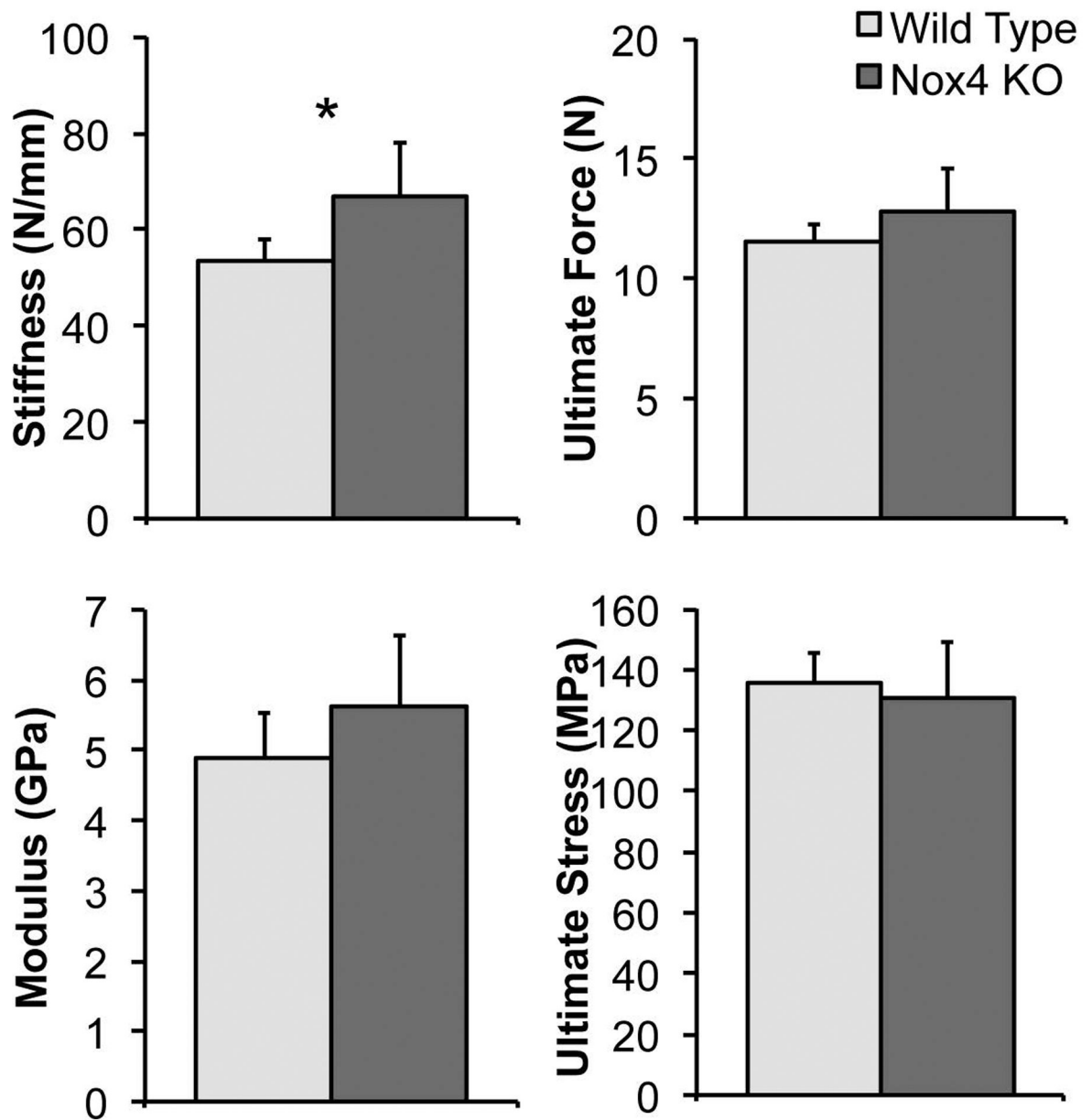


Figure 5.

Mechanical testing of young (10 week old) wild type vs. Nox4 knockout mice. Femurs from WT mice are significantly less stiff, with similar ultimate force, modulus, and ultimate stress in 3-point bending tests. * indicates $p < 0.05$ compared to wild-type.